Capillary-inertial colloidal catapults upon drop coalescence

Roger L. Chavez,[1,a)] Fangjie Liu,[1,a)] James J. Feng,[2,3] and Chuan-Hua Chen[1,b)]
[1]*Department of Mechanical Engineering and Materials Science, Duke University, Durham, North Carolina 27708, USA*
[2]*Department of Mathematics, University of British Columbia, Vancouver, British Columbia V6T 1Z2, Canada*
[3]*Department of Chemical and Biological Engineering, University of British Columbia, Vancouver, British Columbia V6T 1Z3, Canada*

(Received 21 March 2016; accepted 13 May 2016; published online 5 July 2016)

Surface energy released upon drop coalescence is known to power the self-propelled jumping of liquid droplets on superhydrophobic solid surfaces, and the jumping droplets can additionally carry colloidal payloads toward self-cleaning. Here, we show that drop coalescence on a spherical particle leads to self-propelled launching of the particle from virtually any solid surface. The main prerequisite is an intermediate wettability of the particle, such that the momentum from the capillary-inertial drop coalescence process can be transferred to the particle. By momentum conservation, the launching velocity of the particle-drop complex is proportional to the capillary-inertial velocity based on the drop radius and to the fraction of the liquid mass in the total mass. The capillary-inertial catapult is not only an alternative mechanism for removing colloidal contaminants, but also a useful model system for studying ballistospore launching. *Published by AIP Publishing*. [http://dx.doi.org/10.1063/1.4955085]

When two liquid drops coalesce into one, surface energy is released along with the reduction in the overall area of the liquid-gas interface. If the symmetry of drop coalescence is broken by a superhydrophobic substrate, the merged drop can spontaneously jump away from the solid support.[1,2] The self-propelled jumping motion is most often observed during condensation upon the coalescence of growing condensate drops,[3–8] including multiple ones.[9–12] The jumping droplets can additionally carry colloidal contaminants away from the superhydrophobic substrate,[13–15] offering an alternative route to capillarity-driven self-cleaning[16–18] with complete independence to external forces. So far, the decontamination by the self-propelled droplets has only been reported on superhydrophobic surfaces. In this Letter, we show that a colloidal particle can be catapulted away from the supporting surface upon drop coalescence *on the particle*. Our colloidal catapult is inspired by the ballistospore discharge process[19–21] that launches fungal spores upon drop coalescence.[22–24] The bioinspired colloidal catapult is essentially independent of the wettability of the surface to be decontaminated, unlike previously reported mechanisms of decontamination.

As schematically shown in Fig. 1, the colloidal catapult is powered by surface energy released upon drop coalescence on the solid payload. When two drops merge on a partially wetting particle as in Fig. 1(a), a two-stage process leads to the eventual launching. At the first stage, the merged drop acquires a net upward momentum driven by capillarity as in Fig. 1(b). The accelerating drop exerts a downward force on the particle, denoted by the purple arrow, compressing it against the supporting substrate. When the merged drop reaches its peak vertical momentum as in Fig. 1(c), the net force between the drop and the particle is zero at that instant, and the merged drop is at a pseudoequilibrium configuration with a rounded shape (similar to that in Ref. 2). The pseudoequilibrium configuration in Fig. 1(c) demarcates the first and second stages. At the second stage, the merged drop starts to decelerate due to adhesive forces from the solid particle, and an upward force is now exerted on the particle. As long as the particle-substrate adhesion is not too strong, the particle is pulled away from the supporting substrate by capillarity, resulting in the self-propelled catapulting of the particle-drop complex in Fig. 1(d). Here, gravity is neglected since the colloidal particle of interest is much smaller than the millimetric capillary length. It should be noted that the catapulting momentum is ultimately imparted by the supporting substrate which, via the particle, exerts an upward force on the merged drop during its accelerating phase. However, the colloidal removal mechanism in Fig. 1 depends on the wettability of the particle, not the wettability of the supporting substrate as in prior work.

Two necessary conditions should be met for the colloidal catapult in Fig. 1 to function properly, and are indeed satisfied by the experiments and simulations below: (i) The drop coalescence is in the capillary-inertial regime[2] with a small Ohnesorge number, $Oh = \mu_L/\sqrt{\rho_L \sigma r_d} \ll 1$, where μ_L is the liquid viscosity, ρ_L is the liquid density, σ is the

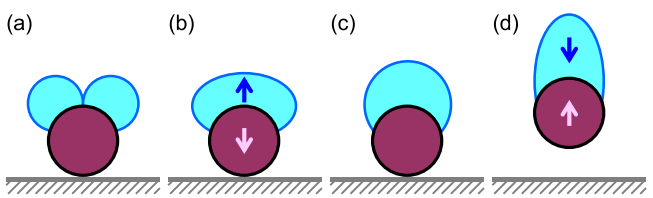

FIG. 1. Capillary-inertial colloidal catapult upon drop coalescence on a particle of intermediate wettability. With the symmetric configuration depicted, the coalescence process only produces net momentum in the vertical direction. The blue (dark) arrow denotes the force exerted on the merged drop by the solid particle, and the purple (light) arrow denotes the counter force on the particle.

[a)]R. L. Chavez and F. Liu contributed equally to this work.
[b)]chuanhua.chen@duke.edu

liquid-gas surface tension, and r_d is the characteristic drop radius prior to coalescence. In the capillary-inertial regime, the merged drop evolves toward the equilibrium shape via many rounds of underdamped oscillations,[25,26] permitting the conversion from the released surface energy to useful kinetic energy. The process is characterized by the capillary-inertial velocity $u_{ci} = \sqrt{\sigma/(\rho_L r_d)}$ and time $\tau_{ci} = \sqrt{\rho_L r_d^3/\sigma}$. (ii) The colloidal particle must exhibit an intermediate wettability with $0^\circ \ll \theta \ll 180^\circ$, where θ is Young's contact angle. On a non-wetting particle with $\theta \approx 180^\circ$, the released energy gives rise to the self-propelled jumping of pure liquid drops that will detach from the particle surface;[3] On a completely wetting particle with $\theta \approx 0^\circ$, surface energy cannot be effectively released with a spreading parameter close to zero.[27] We have demonstrated capillary-inertial catapulting of particles with θ between 60° and 120°, e.g., particles made of polymethyl methacrylate (PMMA) or alkylsilane-coated glass, but the applicable Young's contact angles likely span a larger range.

For the proof of concept, we shall use spherical particles as the payload. Since the spherical shape minimizes the particle-substrate adhesion, the instant of launching is expected to coincide with the pseudoequilibrium point in Fig. 1(c), or shortly afterward in the presence of a small particle-substrate adhesion. At pseudoequilibrium, the vertical drop momentum is at its peak value and the compressive force between the particle and the substrate vanishes. For a spherical particle with negligible adhesion to the substrate, its momentum will simply be given by the peak drop momentum attained at the transition between the first and second stages. It should be noted that the spherical shape is not essential, and a substantial adhesive force can be overcome by the capillary-inertial force associated with the coalescence-induced catapult.[13,28]

The colloidal catapult is experimentally demonstrated in Fig. 2(a). The droplets are produced by an inkjet dispenser with a nozzle radius of 10 μm (MicroFab MJ-AL-01-20-8MX) controlled by a function generator (Agilent 33220A) via a high-voltage amplifier (A. A. Lab A-301HS). Two deionized water drops are sequentially deposited onto an initially dry polystyrene sphere (Norstone 0.3 mm SHC, density $= 1.05$ g/cm^3), which rests on an as-received silicon substrate. In Fig. 2(a), the average drop radius $r_d = 99$ μm, corresponding to a small Ohnesorge number $Oh = 0.0127$ with water properties at 20 °C. For water on polystyrene, the advancing and receding contact angles are $\theta_A/\theta_R = 90^\circ/75^\circ$. The coalescence-induced catapulting is recorded by a high-speed camera (Phantom 7.1 or 710) attached to a long-distance microscope (Infinity K2) with a 10× objective.

The three-dimensional (3D) coalescence process in Fig. 2(a) is qualitatively captured by two-dimensional (2D) simulations in Fig. 2(b). The interfacial simulations follow the procedures outlined in Refs. 2 and 29, except for a small dimensionless mobility of $\gamma^* = 10^{-9}$ which effectively pins the contact line. Due to limitations in our numerical code, we cannot simulate the lift-off and thus the particle remains on the substrate. But this is not a serious drawback as it has no effect until the point of launching, the point when the vertical drop momentum reaches its peak value. As discussed below, this peak momentum is the launching momentum of the drop-particle complex.

The two-stage catapulting process is apparent in Fig. 2(a). During the first stage, the merged drop accelerates upward until around $t = 0.25$ ms, the point of particle departure from the substrate. This point marks the beginning of the second stage, during which the launched particle-drop complex continues to experience internal oscillations, but the overall momentum is conserved. Despite the stationary particle in Fig. 2(b), the numerical evolution of drop shapes agrees well with the experimental process in Fig. 2(a). Most importantly, the numerical drop momentum peaks at $t^* = 1.94$ for the $r_d/r_p = 0.67$ case in Fig. 3(a), in good agreement with the experiential point of launching at $t = 0.25 \pm 0.05$ ms ($t^* = 2.18 \pm 0.44$) in Fig. 2(a). For a spherical catapult with symmetric coalescence, we identify

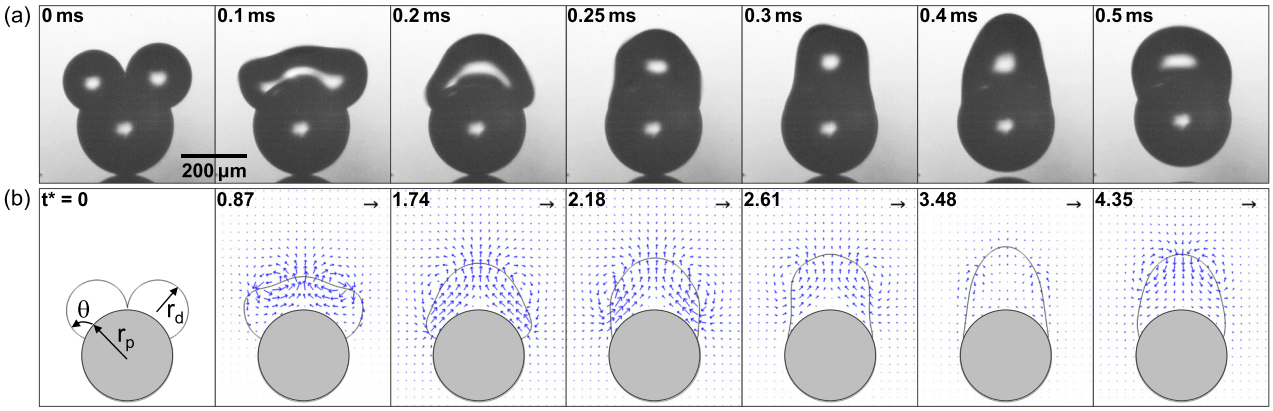

FIG. 2. Drop coalescence process leading to colloidal catapulting: (a) Coalescence of water drops ($r_d = 99$ μm) on a polystyrene particle ($r_p = 148$ μm), which is surrounded by air and supported by a silicon substrate. Since the particle-substrate contact is already slightly reduced at 0.3 ms (more apparent in the video), the particle departure from the substrate must have started at 0.25 ± 0.05 ms, at which point the merged drop starts to exert an upward force to pull the particle away from the substrate. (b) 2D simulations of symmetric drop coalescence on a stationary particle, where the unit vectors represent the capillary-inertial velocity u_{ci} and the time is reduced by the capillary-inertial time with $t^* = t/\tau_{ci}$. The numerical parameters are adopted to match the experiments in (a): $Oh = 0.0127$, $r_d/r_p = 0.67$, and $\theta = 90^\circ$. A small mobility parameter of $\gamma^* = 10^{-9}$ is chosen to effectively pin the contact line. Other properties including the water and air properties at 20 °C can be found in Liu *et al.*[2] (Multimedia view) [URL: http://dx.doi.org/10.1063/1.4955085.1] [URL: http://dx.doi.org/10.1063/1.4955085.2]

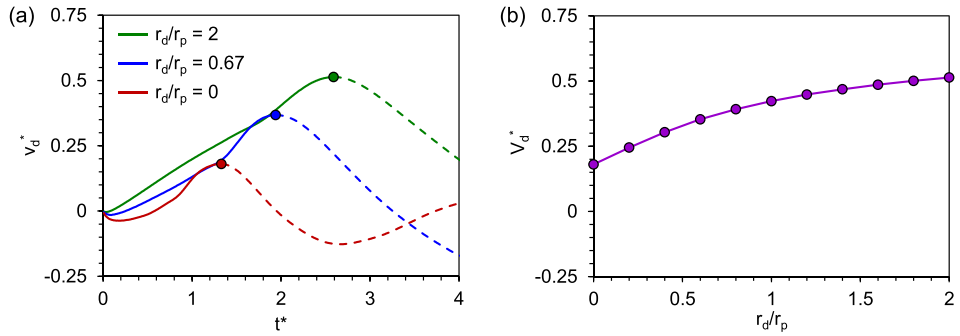

FIG. 3. Dependence of the simulated drop velocity on the drop-to-particle radius ratio r_d/r_p. (a) Evolution of the mass-averaged drop velocity $v_d^* = v_d/u_{ci}$ for different r_d/r_p under otherwise identical conditions. The $r_d/r_p = 0.67$ case corresponds to Fig. 2(b). The $v_d^*(t^*)$ curves obtained on the fixed particle are physically meaningful for the solid-line portions, up to the peak velocity V_d^* indicated by dots. Beyond the peak velocity, the particle is catapulted away. (b) The simulated peak velocity V_d^* is a weak function of r_d/r_p. The V_d^* in (b) is the peak value from the corresponding $v_d^*(t^*)$ curve in (a).

the point of launching with the instant of peak drop momentum, or the pseudoequilibrium configuration with zero overall acceleration as in Fig. 1(c).

Motivated by the two-stage catapulting process, a scaling model is derived for the catapulting velocity of the particle-drop complex. During the first stage, the particle remains stationary but the merged drop is driven to move upward by the surface energy released during the merging process. At the end of the first stage, the (vertical) velocity averaged over the liquid mass reaches a maximum. By dimensional analysis, this maximum drop velocity V_d is reduced to

$$V_d = V_d^* u_{ci} = V_d^*\left(\mathrm{Oh}, \theta, \frac{r_d}{r_p}\right)\sqrt{\frac{\sigma}{\rho_L r_d}}, \tag{1}$$

where the properties of the surrounding air are not included because of its negligible role.[2] For the nondimensional velocity V_d^* in this study, the Ohnesorge number drops out of the problem in the capillary-inertial regime with $\mathrm{Oh} \ll 1$, and the contact angle is restricted to $\theta \approx 90°$ which is about the optimal contact angle for the colloidal catapult with symmetric coalescence. Under these conditions, V_d^* is mainly a function of r_d/r_p, the radius ratio accounting for the influence of the curved particle boundary when compared to a flat surface (with $r_d/r_p = 0$). The $V_d^*(r_d/r_p)$ dependence is relatively weak as in Fig. 3(b), given that $r_d/r_p \sim 1$ for colloidal catapults in typical scenarios. With the weak dependence on curvature, V_d is proportional to the capillary-inertial velocity u_{ci}, which is based on the initial drop radius r_d.

During the second stage, there is no longer any force exerted on the particle-drop complex, and the peak drop momentum acquired at the end of the first stage is conserved. This momentum is redistributed over the entire mass of $m_{pd} = m_p + m_d$, where m_p is the mass of the particle and m_d is the liquid mass merged from the two initial drops. The catapulting velocity V_{pd} of the particle-drop complex is given by momentum conservation

$$m_{pd} V_{pd} = m_d V_d. \tag{2}$$

The catapulting velocity V_{pd} can be further reduced to

$$V_{pd}^* = \frac{V_{pd}}{u_{ci}} = \frac{V_d}{u_{ci}}\frac{m_d}{m_p + m_d} = V_d^* m^*. \tag{3}$$

The nondimensional catapulting velocity V_{pd}^* is therefore proportional to m^*, the fraction of liquid mass in the total launched mass. One caveat is that in reality m^* is most easily varied by changing r_d/r_p, but the radius ratio has a weak effect on V_d^* shown in Fig. 3(b).

The above scaling model of the two-stage launching process is tested in Fig. 4. The colloidal catapult is triggered by drop coalescence produced by inkjet printing as in Fig. 2(a). The vertical catapulting velocity is measured by tracking the geometrical centroid of the projected image of the particle-drop complex, and the gravitational deceleration is corrected following procedures in Ref. 30. The horizontal launching velocity is much smaller than the vertical one, except for conditions with a marginal vertical velocity. The horizontal velocity component is neglected in Fig. 4, in keeping with the approximately symmetric coalescence around the vertical axis of the solid sphere. Drop and particle volumes are calculated from microscopically measured dimensions. The measurements fit well with a linear relationship $V_{pd}^* = 0.26 m^*$ in accordance with Eq. (3). Note that the linearity holds because of an approximately constant V_d^*. The near constancy of V_d^* can be appreciated from the 2D simulations in Fig. 3(b): the maximum drop velocity V_d^* varies by approximately 30% for $r_d/r_p = 0.38$–0.83, the experimental

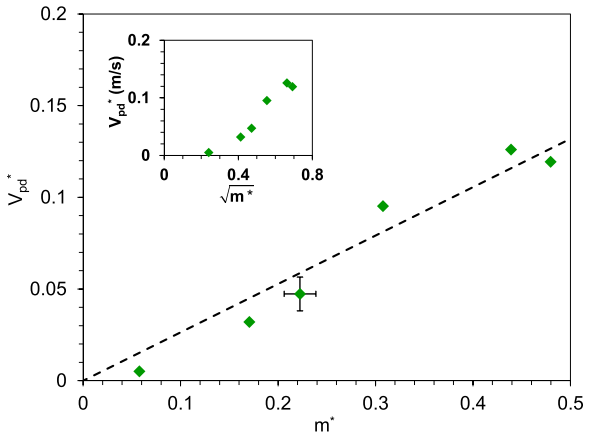

FIG. 4. The nondimensional catapulting velocity V_{pd}^* is proportional to the liquid mass fraction m^* in accordance with Eq. (3). On polystyrene particles with $r_p = 135 \pm 15\ \mu$m, drop coalescence is produced by inkjet printing as in Fig. 2(a) with $r_d/r_p = 0.38$–0.83 ($m^* = 0.06$–0.48). The measurements scatter around $V_{pd}^* = 0.26 m^*$ (the dashed line). In the inset, V_{pd}^* is apparently not a linear function of $\sqrt{m^*}$.

range of radius ratio in Fig. 4. In contrast, the mass fraction m^* varies by 700% in the same range. As a comparison to the two-stage model, a more naive model is tested in the inset of Fig. 4, where the kinetic energy of the launched particle-drop complex is directly related to the released surface energy with $m_{pd}V_{pd}^2 \sim \sigma r_d^2$. This lumped model yields an incorrect relationship $V_{pd}^* \sim \sqrt{m^*}$, which is not supported by the experiments.

Our colloidal catapult is inspired by the ballistospore launching mechanism, where a similar two-stage process is believed to be responsible for launching certain fungal spores.[23,24] A two-stage model incorporating the momentum conservation Eq. (2) has been proposed for ballistospores by Noblin *et al.*,[23] but has not been fully tested because of the limited data on fungal spores, as well as the limited understanding of the fluid dynamics governing the prefactor V_d^*. Our colloidal catapult offers a much simpler and more reproducible system to test the scaling model in Eq. (3).

In addition to being a useful model system for ballistospore discharge, our work also points to an alternative mechanism for removing colloidal contaminants. Like the ballistospore mechanism, the colloidal catapult is particularly useful in the context of condensation, during which surface energy is readily available on droplets that are spontaneously nucleating, growing and coalescing. A representative colloidal catapult upon exposure to condensing vapor is shown in Fig. 5. The colloidal payload is a soda-lime particle (Cospheric P2050SL-S2-2.5, density = 2.5 g/cm^3), silanized to be hydrophobic by the vendor. The particle is catapulted away from the Teflon substrate (polytetrafluoroethylene sealant tape) when two growing condensate drops coalesce together. Because of the smaller drops, the catapulting process governed by the capillary-inertial time (τ_{ci}) is much shorter than that in Fig. 2, although both cases are governed by the same capillary-inertial process following drop coalescence.

A few limitations of our present work are worth noting. (i) The adhesive force between the particle and the substrate is neglected, but some adhesion is expected, e.g., of electrostatic, van der Waals, or capillary origins.[13,28] In fact, a finite adhesive force is probably at play in Fig. 2(a), since it takes an appreciable duration (about 0.05 ms) to completely detach the particle from the supporting substrate. Such an adhesive force will delay the point of launching depicted in Fig. 1(c) and complicate the momentum transfer argument in Eq. (2). The finite adhesion may also explain the offset in Fig. 4, where the coalescing drops need to be large enough for the released surface energy to overcome the adhesion. (ii) The effect of particle and substrate wettability remains to be fully explored. For the particle, an intermediate wettability is necessary for colloidal catapulting, which may pose limits for self-cleaning applications involving particles of wide-ranging wettabilities. For the substrate supporting the particle, the wettability is not of direct relevance. However, if the substrate is hydrophilic (e.g., an untreated glass slide), an appreciable capillary bridge may form between the particle and the substrate in a condensing environment, and the resulting capillary adhesion may prohibit the particle from catapulting away. (iii) The numerical simulations are two-dimensional, preventing quantitative comparison with experimental results. With three-dimensional simulations, the numerically computed average drop velocity V_d^* can be directly compared to that extracted from the experimentally measured $V_{pd}^*(m^*)$ relation. The 3D simulations will facilitate the exploration of the large parametric space governing V_d^*, as in Eq. (1).

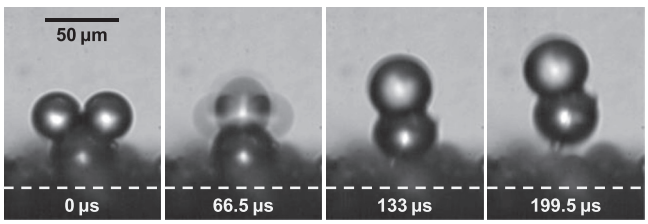

FIG. 5. Colloidal catapulting upon exposure to a condensing water vapor. Upon coalescence of two condensate drops on a hydrophobized glass particle, the particle is removed from the underlying teflon substrate. The particle radius $r_p = 21\ \mu$m and average drop radius $r_d = 17\ \mu$m. (Multimedia view) [URL: http://dx.doi.org/10.1063/1.4955085.3]

In summary, we have demonstrated a colloidal catapult resulting from drop coalescence in the capillary-inertial regime. Experiments and simulations are combined to elucidate the two-stage catapulting process, giving rise to a simple scaling model of the catapulting velocity in Eq. (3). In the first stage, the merged drop gains increasing momentum from the surface energy released upon coalescence, but the particle remains stationary. In the second stage, the decelerating drop pulls the particle away from the supporting substrate by capillarity. The catapulting velocity is proportional to the capillary-inertial velocity and the liquid mass fraction, arising from the surface energy release in the first stage and the momentum conservation in the second stage. The colloidal catapult not only offers a model system to investigate the interfacial flow dynamics underlying ballistospore discharge, but also provides an alternative mechanism to remove colloidal contaminants almost independently of the wettability of the surface to be decontaminated.

This work was supported by the National Science Foundation's Research Triangle MRSEC (DMR-1121107). R.L.C. was supported by the National Institutes of Health via Duke's Center for Biomolecular and Tissue Engineering (T32-GM008555). J.J.F. was supported by the Natural Sciences and Engineering Research Council of Canada. The authors are grateful to M. C. Grobinski and K. Zhang for constructing the inkjet printing system, and to H. Mehrabian, S. N. Patek, A. Pringle, and X. Qu for helpful discussions.

[1]J. B. Boreyko and C. H. Chen, Phys. Rev. Lett. **103**, 184501 (2009).
[2]F. Liu, G. Ghigliotti, J. J. Feng, and C. H. Chen, J. Fluid Mech. **752**, 39 (2014).
[3]M. Kollera and U. Grigull, Heat Mass Transfer **2**, 31 (1969).
[4]C. H. Chen, Q. Cai, C. Tsai, C. L. Chen, G. Xiong, Y. Yu, and Z. Ren, Appl. Phys. Lett. **90**, 173108 (2007).
[5]C. Dietz, K. Rykaczewski, A. Fedorov, and Y. Joshi, Appl. Phys. Lett. **97**, 033104 (2010).
[6]J. Feng, Z. Qin, and S. Yao, Langmuir **28**, 6067 (2012).
[7]M. He, X. Zhou, X. Zeng, D. Cui, Q. Zhang, J. Chen, H. Li, J. Wang, Z. Cao, Y. Song, and L. Jiang, Soft Matter **8**, 6680 (2012).
[8]N. Miljkovic, R. Enright, Y. Nam, K. Lopez, N. Dou, J. Sack, and E. N. Wang, Nano Lett. **13**, 179 (2013).
[9]K. Rykaczewski, A. T. Paxson, S. Anand, X. Chen, Z. Wang, and K. K. Varanasi, Langmuir **29**, 881 (2013).

[10]J. Tian, J. Zhu, H.-Y. Guo, J. Li, X.-Q. Feng, and X. Gao, J. Phys. Chem. Lett. **5**, 2084 (2014).
[11]X. Chen, J. A. Weibel, and S. V. Garimella, Adv. Mater. Interfaces **2**, 1400480 (2015).
[12]X. Qu, J. B. Boreyko, F. Liu, R. L. Agapov, N. V. Lavrik, S. T. Retterer, J. J. Feng, C. P. Collier, and C. H. Chen, Appl. Phys. Lett. **106**, 221601 (2015).
[13]K. M. Wisdom, J. A. Watson, X. Qu, F. Liu, G. S. Watson, and C. H. Chen, Proc. Natl. Acad. Sci. U. S. A. **110**, 7992 (2013).
[14]G. S. Watson, M. Gellender, and J. A. Watson, Biofouling **30**, 427 (2014).
[15]G. S. Watson, L. Schwarzkopf, B. W. Cribb, S. Myhra, M. Gellender, and J. A. Watson, J. R. Soc. Interface **12**, 20141396 (2015).
[16]W. Barthlott and C. Neinhuis, Planta **202**, 1 (1997).
[17]A. Nakajima, K. Hashimoto, T. Watanabe, K. Takai, G. Yamauchi, and A. Fujishima, Langmuir **16**, 7044 (2000).
[18]S. Nishimoto and B. Bhushan, RSC Adv. **3**, 671 (2013).
[19]A. H. R. Buller, *Researches on Fungi* (Green and Company, London, 1909–1950), Vol. 1–7.
[20]J. Webster, R. A. Davey, G. A. Duller, and C. T. Ingold, Trans. Br. Mycol. Soc. **82**, 13 (1984).
[21]N. P. Money, Mycologia **90**, 547 (1998).
[22]A. Pringle, S. N. Patek, M. Fischer, J. Stolze, and N. P. Money, Mycologia **97**, 866 (2005).
[23]X. Noblin, S. Yang, and J. Dumais, J. Exp. Biol. **212**, 2835 (2009).
[24]F. Liu, R. L. Chavez, S. N. Patek, A. Pringle, J. J. Feng, and C. H. Chen, "Asymmetric drop coalescence controls the capillary-inertial launching of fungal ballistospores," Proc. Natl. Acad. Sci. U. S. A. (submitted).
[25]L. Rayleigh, Proc. R. Soc. London **29**, 71 (1879).
[26]S. Chandrasekhar, *Hydrodynamic and Hydromagnetic Stability* (Dover, 1961).
[27]P.-G. de Gennes, Rev. Mod. Phys. **57**, 827 (1985).
[28]J. Visser, Part. Sci. Technol. **13**, 169 (1995).
[29]K. Zhang, F. Liu, A. J. Williams, X. Qu, J. J. Feng, and C. H. Chen, Phys. Rev. Lett. **115**, 074502 (2015).
[30]F. Liu, G. Ghigliotti, J. J. Feng, and C. H. Chen, J. Fluid Mech. **752**, 22 (2014).